Supplementary Information: Canopy-Mediated Climate Feedbacks in the Boreal Continuous Permafrost Zone

S.M. Stuenzi[1,2*], G. Grosse[2,3], F. Miesner[2,4], S. Westermann[4,5], M. Langer[6,2]

[1*]Geography Department, Humboldt-Universität zu Berlin, Unter den Linden 6, Berlin, 10099, Berlin, Germany.
[2]Permafrost Research Section, Alfred Wegener Institute Helmholtz Centre for Polar and Marine Research, Telegrafenberg A45, Potsdam, 14473, Brandenburg, Germany.
[3]Institute of Geosciences, University of Potsdam, Karl-Liebknecht-Strasse 24-25, Potsdam, 14476, Brandenburg, Germany.
[4]Department of Geosciences, University of Oslo, Sem Slands vei 1, Oslo, 0316, State, Norway.
[5]Centre for Biogeochemistry in the Anthropocene, University of Oslo, Sem Slands vei 1, Oslo, 0316, State, Norway.
[6]Department of Earth Sciences, Vrije Universiteit Amsterdam, De Boelelaan 1085, Amsterdam, 1081 HV, State, The Netherlands.

*Corresponding author(s). E-mail(s): simone.maria.stuenzi.1@hu-berlin.de;
Contributing authors: guido.grosse@awi.de; frederieke.miesner@awi.de; sebastian.westermann@geo.uio.no; moritz.langer@awi.de;

S1 Comparison to field measurements and model-derived data sets

To evaluate our simulated ALT differences between forested and unforested conditions, we compare our results with field measurements and model-based estimates. Our approach prioritizes capturing regional variability and relative changes rather than fine-scale spatial detail or absolute depths. The simulated ALTs show generally good agreement with Circumpolar Active Layer Monitoring (CALM) measurements across the three clusters [1], where measurements are available, despite sparse observational data in forested continuous permafrost regions (Fig. 1). When compared to the spatially explicit ESA CCI ALT dataset [2], our forested simulations generally fall within the range and cluster around median values in 13 out of 15 cases, while our bare ground simulations consistently exceed the range (Fig. 1). The ALT product is derived from CryoGrid simulations driven by MODIS Land Surface Temperature merged with downscaled ERA5 reanalysis data and constrained by landcover satellite observations. While the product incorporates landcover-dependent snow parameterizations, it does not account for physical canopy effects. The large tails in CCI distributions reflect multiple landcover types modeled within heterogeneous grid cells. Differences between our simulated ALT and CGLite model outputs become particularly apparent in the southern regions of the continuous permafrost zone. CGLite, which initiates simulations around year 500 CE without explicit vegetation effects, does not simulate permafrost in these areas, as the model does not account for ecosystem-protected permafrost [3]. This leads to systematic absence of permafrost near the southern margins in CGLite results. In contrast, our analysis utilizes the permafrost zonation dataset by Obu et al. (2019) [4], which captures ecosystem-protected permafrost but also carries its own limitations and uncertainties in spatial delineation. These discrepancies highlight how model assumptions and input datasets fundamentally influence permafrost extent projections, especially near the margins of continuous permafrost zones where ecosystems are critical for permafrost persistence. Our simulated ALT differences between forested and bare ground conditions (δALT = 0.9–1.4 m) partly exceed those reported in a recent synthesis of pre- and post-fire active layer depths in continuous permafrost zones (up to 1.1 m) [5]. This discrepancy is expected for two reasons: (1) the synthesis includes varying burn severities with incomplete canopy removal, while our bare ground simulations represent complete vegetation absence; and (2) the synthesis dataset underrepresents Russian sites [5].

Several limitations constrain absolute ALT validation in our study. Our simulations represent cluster-scale averages using broad climatic proxies rather than site-specific conditions, while CALM measurements are point-based. The coarse spatial resolution of climate zones, static plant functional type assignments, uniform leaf area index within clusters, and absence of soil stratigraphic variability limit our ability to capture finer-scale landscape heterogeneity. This explains poorer agreement in the two smallest clusters (evergreen needleleaf in BSk and deciduous needleleaf in Dsc climate zones in NA). Additionally, the CCI Permafrost dataset exhibits substantial uncertainty in ALT, which is its least constrained variable. Despite these limitations, our focus on relative changes between forested and bare ground conditions provides a robust basis for assessing canopy thermal buffering effects on permafrost carbon vulnerability, as the systematic bias in absolute depths cancels out when calculating differences.

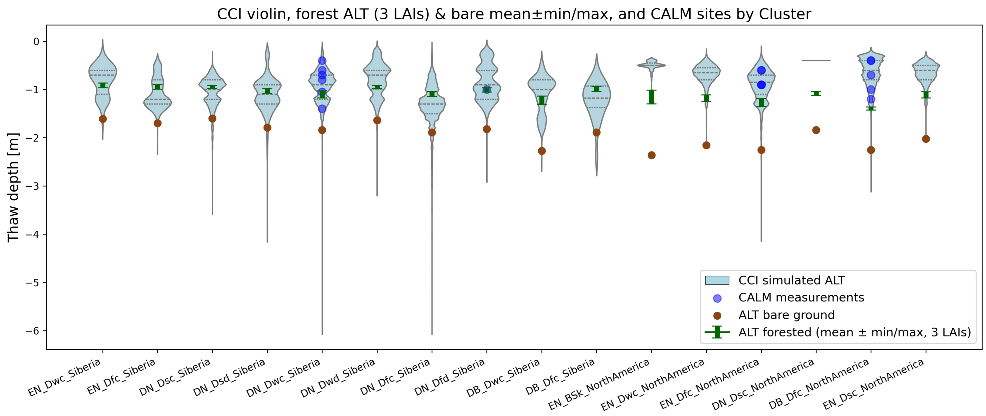

Fig. 1 Violin plots showing probability densities of model-based estimates of cluster-wise ALTs (light blue, [2]), with overlaid points from forested simulations (ForestedALT, green) and bare ground simulations (BareALT, orange). Blue circles denote in-situ CALM measurements [1]. Violins depict kernel-smoothed distributions with quartile markers (inner lines).

S2 Forest canopy effects on permafrost thaw depth

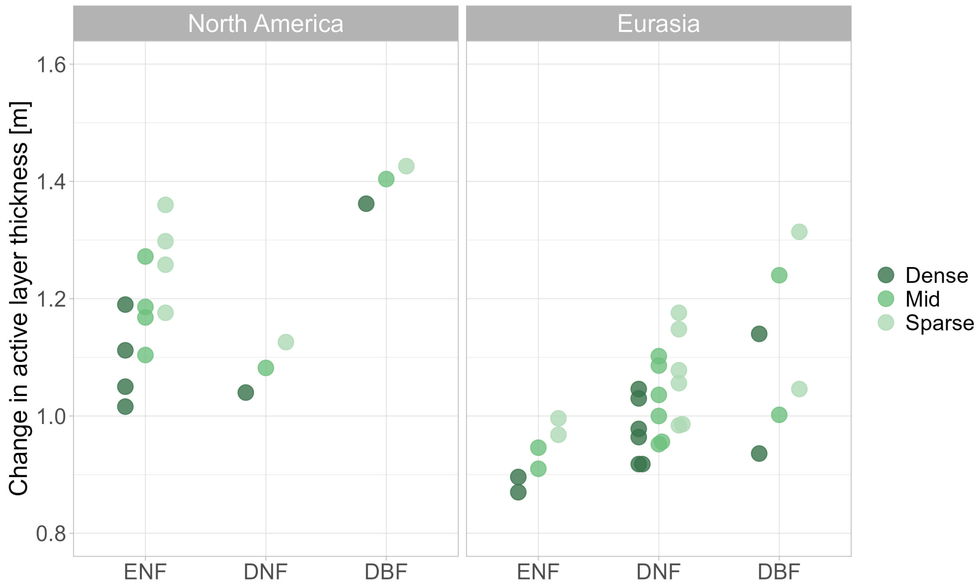

Fig. 2 Forest canopy effects on permafrost thaw depth. ALT change between forested and bare ground simulations across (1) PFTs and (2) forest density categories (sparse: LAI = $1\,m^2\,m^{-2}$; mid: LAI = $2\,m^2\,m^{-2}$; dense: LAI = $4\,m^2\,m^{-2}$) in NA and Eurasian boreal regions.

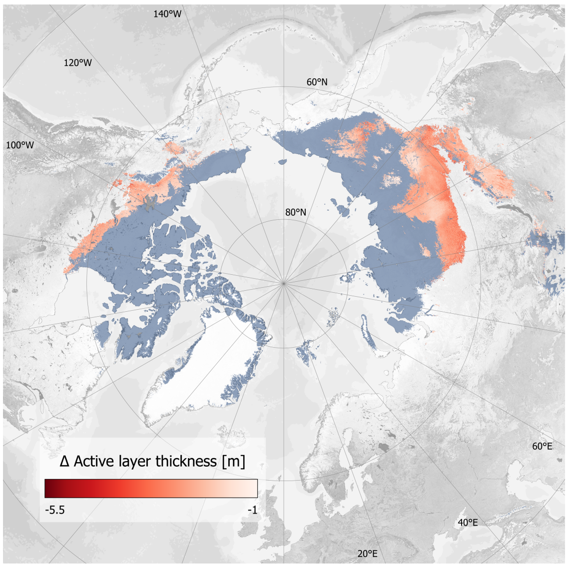

Fig. 3 Spatial distribution of active layer thickness under simulated bare ground conditions across boreal continuous permafrost regions. Map showing the active layer thickness for bare ground conditions, calculated by subtracting the forest-induced ALT reduction (sparse scenario) from the baseline permafrost ALT. The resulting values represent the potential ALT in the absence of boreal forest cover.

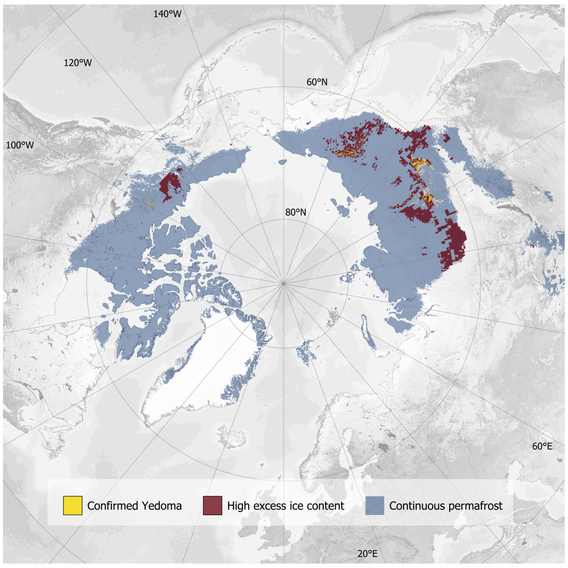

Fig. 4 High ground ice content and confirmed Yedoma extent. Map showing the spatial distribution of high ground ice content based on the Circum-Arctic Map of Permafrost and Ground-Ice Conditions, V2 [6] and confirmed Yedoma extent [7, 8] in forested continuous permafrost.

Table 1 Comparison of the effect of the temporal averaging of simulation output. The comparison of 3-, 5-, and 10-year averaging windows reveals differences in modeled ALT across climate zones and PFTs. Longer averaging periods generally reduce the metric values, suggesting that interannual variability is considerable in some clusters. The 5-year averaging window was selected as a compromise between capturing interannual dynamics and reducing noise from extreme years, providing intermediate values between the 3- and 10-year averages. Some region-PFT-climate combinations show relatively high sensitivity to the averaging period (e.g., Eurasian DNF in Dfc, Dsc, and Dsd climates, and North American ENF in Dsc and Dwc), as the 5-year window may not fully smooth the interannual variability. Conversely, combinations showing minimal sensitivity to averaging period (e.g., Eurasian DNF in Dwc) appear more temporally stable.

Region	PFT	CZ	3-year mean	5-year mean	10-year mean
Eurasia	ENF	Dwc	0.913	0.910	0.907
Eurasia	ENF	Dfc	0.950	0.946	0.922
Eurasia	DNF	Dsc	0.950	0.952	0.916
Eurasia	DNF	Dwd	0.963	0.956	0.931
Eurasia	DNF	Dfd	1.000	1.000	0.996
Eurasia	DBF	Dfc	1.017	1.002	0.991
Eurasia	DNF	Dsd	1.047	1.036	1.004
NorthAmerica	DNF	Dsc	1.067	1.082	1.093
Eurasia	DNF	Dwc	1.097	1.086	1.086
NorthAmerica	ENF	Dsc	1.100	1.104	1.061
Eurasia	DNF	Dfc	1.110	1.102	1.097
NorthAmerica	ENF	BSk	1.203	1.186	1.151
NorthAmerica	ENF	Dwc	1.230	1.168	1.137
Eurasia	DB	Dwc	1.240	1.240	1.241
NorthAmerica	ENF	Dfc	1.277	1.272	1.267
NorthAmerica	DBF	Dfc	1.407	1.404	1.398

S3 Size and vulnerability of carbon pools in NH permafrost regions

Table 2 Size of carbon pools in NH permafrost regions. Values show SOC stocks (in Pg C) and their fractional distribution across permafrost zones. "Frozen due to canopy" refers to SOC stabilized by forest insulation, while "vulnerable to rapid-thaw" indicates additional deeper SOC at risk from abrupt permafrost degradation upon deforestation in ice-rich areas. LAI scenarios (1, 2, 4) reflect sparse, medium, and dense LAIs, respectively. Sources integrate land cover data [9], permafrost zonation [4], simulated active layer depths [2], ground ice conditions [6], and soil carbon datasets [7].

Carbon Pool	SOC (Pg C)	% of Total	% of PF Frozen	Source
Within Permafrost Region				
Total	1238.2	100.0	–	[4, 7]
Frozen	915.3	73.9	100.0	[2]
Seasonally thawed	322.9	26.1	–	[2]
Within Forested Continuous Permafrost				
Total	183.1	14.8	–	[4, 9]
Frozen	117.9	–	12.9	[2]
Seasonally thawed	65.2	–	–	[2]
Canopy-mediated SOC	39.5	3.2	4.3	
Sparse LAI	41.1	–	–	
Medium LAI	39.5	–	–	
Dense LAI	37.9	–	–	
Rapid-thaw affected SOC	19.3	1.6	2.1	[6]
Sparse LAI	17.7	–	–	
Medium LAI	19.3	–	–	
Dense LAI	20.9	–	–	
Total Vulnerable to Thaw	58.8	4.8	6.4	

Table 3 SOC stocks and vulnerability across major forested continuous permafrost soil classes. Reported for each soil class are the estimated SOC stocks (in Pg), relative areal coverage (percentage of forested continuous permafrost area), and qualitative assessment of the vulnerability to thaw. Vulnerability classifications are based on susceptibility to permafrost degradation and carbon release. Data from [7, 8].

Class	Vulnerability	SOC [Pg]	Percent of area [%]
Yedoma	Very high	1.7	4.8
Turbel	High	15	32.6
Orthel	Medium	17	48.6
Histel	Low	6.4	8.9
Histosol	Low	0.3	0.5
Unknown soil class	unknown	0.9	4.5

S4 Extended discussion

S4.1 Land-use changes

The critical role of permafrost and vegetation in protecting soil carbon is further emphasized by land-use change studies. Empirical evidence from permafrost-affected forest soils in the Yukon highlight the crucial role of permafrost presence and land-use change in shaping SOC dynamics. Sampling across 18 farms spanning permafrost and non-permafrost soils, revealed that conversion of forest to cropland and grassland on permafrost soils resulted in significant SOC losses, approximately 15.6±21.3% and 23.0±13.0%, respectively [10]. In deforested soils permafrost was absent while soils without previous permafrost showed no significant SOC loss and, in some cases, slight SOC gains under grassland. The study also found that land-use change caused marked carbon losses in organic soils, while carbon associated with mineral soils increased. These results demonstrate that the response of SOC to deforestation strongly depends on initial permafrost abundance, governed more by climatic than soil properties [10]. These findings are echoed across the boreal zone. In Alaska, agricultural development led to ecosystem carbon losses of up to 31 $kg\,m^{-2}$, nearly 70%, within just six years on permafrost soils, compared to 11 $kg\,m^{-2}$ (34%) on non-permafrost soils over several decades [11]. Such losses are far more rapid than long-term projections from warming or wildfire alone, which estimate 5–6 $kg\,m^{-2}$ of carbon loss over 500 years. Deforestation in boreal chronosequences shows similarly large impacts: agricultural soils were found to hold 44% less carbon than their forested counterparts, equivalent to an average loss of 8.3 $kg\,m^{-2}$ [12]. While some logged forests show short-term recovery of soil carbon and nitrogen, long-term carbon cycling remains disrupted for decades to centuries [11]. Moreover, conversion of northern lands to agriculture accelerates the mineralization of soil carbon, especially in the upper meter of soil, and warming-driven gains in net primary production cannot offset these losses [13]. Isotopic and biochemical evidence confirms these patterns: permafrost thaw reduces surface SOC stocks by up to 50% within the top 0.125 m, with signs of increased microbial decomposition and declining C:N ratios [14]. In northern Sweden, bulk δ^{14}C values have been shown to mask the degradation of aged, highly biodegradable carbon pools, underscoring the need for more nuanced detection methods [15].

S4.2 Disturbances

The thermal protection capacity is increasingly undermined by disturbances. Pressures are intensifying from both natural disturbances as well as expanding human activities including logging and agricultural conversion [16, 17]. Warming temperatures, heatwaves, drying, and earlier snowmelt are accelerating both the frequency and severity of disturbances, with projections indicating future escalation [18–20]. Some disturbance regimes exhibit strong positive feedbacks: disturbance-accelerated permafrost thaw leads to ground drying, thermokarst formation, and enhanced susceptibility to biotic stressors, further destabilizing forest cover and hydrothermal ground conditions [21, 22]. Recent findings suggest covariation of forest carbon balance with forest age and an increasing shift towards younger forest stands with lower aboveground carbon stocks due to higher frequency disturbances [23]. The relationship between canopy structure and thermal protection is non-linear, with implications for understanding partial disturbance impacts. Sparser canopies exhibit slightly stronger buffering per unit area 2, reflecting a delicate balance between competing processes: while denser canopies provide greater shading, they also enhance evapotranspiration that can dry soils and increase ALT. This suggests that moderate canopy thinning from drought stress, insect damage, or selective logging may not immediately compromise thermal protection in proportion to canopy loss. However, even partial canopy removal or density changes have substantial impacts on active layer and permafrost hydrothermal conditions [24–26], and the non-linear response complicates predictions of carbon vulnerability under gradual forest degradation. Critically, this also means that landscapes experiencing chronic stress, such as drought-induced canopy dieback or partial insect defoliation, may cross thresholds of permafrost destabilization before complete forest loss occurs, mobilizing the carbon pools quantified above through incremental rather than catastrophic change.

Wildfire represents the most immediate and widespread disturbance, with impacts operating across multiple timescales. Fire combusts biomass and near-surface SOC, directly transferring carbon and nitrogen to the atmosphere [27], but the longer-term thermal destabilization of deeper permafrost stocks may be more consequential. Fire accelerates active-layer deepening and soil warming by removing both the insulating organic layer and the canopy [26]. In burned and subsided soils, carbon pools in the upper 1.25 m are reduced by more than half (from $7.3\,\mathrm{kg\,m^{-2}}$ to $3.1\,\mathrm{kg\,m^{-2}}$), with only approximately 10 % lost during combustion and the remainder through subsequent thaw-driven microbial decomposition [14, 28, 29].

Wind damage and insect outbreaks, intensified by climatic stressors, cause widespread tree mortality that creates deadwood fueling subsequent fires and pathogen attacks, with cascading interactions triggering compounding impacts on soil thermal stability and carbon release [30–32]. Changes in species composition, such as shifts towards broadleaf deciduous taxa that are less fire-prone, may partially counteract some feedbacks, although resilience is limited under rapidly changing disturbance regimes [33].

In Yedoma regions, disturbances can destabilize ice wedge networks, triggering thermokarst collapse that rapidly mobilizes millennia-old carbon and nitrogen, representing a powerful pathway for long-term SOC loss and permafrost-climate amplification [34, 35]. The interacting impacts of fire and Yedoma thaw on coupled carbon-nitrogen pools remain poorly constrained, though isotopic evidence provides initial indications of strongly altered biogeochemistry [14, 36]. Isotopic shifts (δ^{13}C enrichment) and declining C:N ratios signal intensified decomposition and altered nutrient cycling. Associated losses in total and labile nitrogen, along with depletion in foliar nitrogen, underscore that disturbance destabilizes both carbon and nitrogen reservoirs [14].

S4.3 Vegetation Feedback and Carbon Sequestration

Potential carbon release is influenced by vegetation changes, which may offset some soil carbon losses through increased growth and carbon uptake [37]. For instance, elevated atmospheric CO_2 and higher temperatures can stimulate boreal forest greening, potentially compensating for soil carbon declines this century according to some models [38]. Enhanced nitrogen availability from mineralization and newly thawed dissolved nitrogen can further boost plant productivity if the excess nitrogen is retained in the soil rather than lost to leaching or denitrification [39, 40]. The balance between soil carbon decomposition and vegetation regrowth depends critically on disturbance regimes, post-disturbance succession trajectories such as shifts in dominant tree species, and climatic trends [41–43]. However, increased plant growth does not necessarily translate into greater ecosystem carbon storage. For example, enhanced root-derived carbon inputs can stimulate microbial decomposition of existing soil carbon through priming effects, potentially offsetting gains [44]. Moreover, changes in vegetation type, such as shrub or tree expansion into tundra or changes in tree species composition, interact with snow cover, soil temperatures, and microbial activity in complex ways, and it remains unclear whether such changes increase or decrease soil carbon stocks [42, 45–47]. As such, the expansion of highly productive birch forest into tundra heath has been found to stimulate the decomposition of older soil organic matter through positive priming effects associated with high plant activity during the growing season. This process may lead to lower soil carbon storage in forested areas despite higher productivity, and suggests that forest colonization of tundra could accelerate the release of large tundra soil carbon stocks to the atmosphere [48]. Nevertheless, ongoing and future climatic change might lead to exceeding tolerance thresholds of boreal plant species, leading to increased mortality and limited seed dispersal which could impact the vegetation communities for centuries [49]. Consistent with decadal biomass trends in boreal forests, net carbon gains may initially occur through densification of sparse northern forests, offsetting thinning in southern stands [50]. However, this aboveground carbon accumulation would eventually plateau due to density-dependent growth limitations and limited land areas for expansion currently dominated by tundra. While warming-induced permafrost retreat could facilitate forest expansion in northern boreal regions, the thaw and decomposition of the frozen SOC in NH permafrost, a pool 10–20 times larger than boreal biomass stocks, would exceed any vegetation carbon gains across most of the biome [51]. Furthermore, after the onset of net-zero and negative emissions scenarios, vegetation carbon stocks stabilize or decline due to the decreased CO_2 fertilization effects, while soil carbon losses continue due to soil respiration, resulting in a net ecosystem carbon loss [52], additionally highlighting the differences in carbon pool vulnerabilities and sizes.

S4.4 Uncertainties

Our first-order estimates are subject to methodological uncertainties that reflect current data and process representation limitations. Most SOC assessments sample only to 1 m depth [53], potentially missing deeper stores especially found in permafrost soils [54–56]. Total boreal region carbon estimates span a nearly five-fold range from 367.3–1715.8 Pg [57, 58], when including vegetation, soil, and peatland carbon, reflecting methodological inconsistencies and spatial heterogeneity. Deadwood remains particularly uncertain, ranging from 15–25% of aboveground biomass in undisturbed stands to 40–60% post-fire in larch forests [59]. Further uncertainties arise from potential inclusion of biomass components in the SOC estimates from the Northern Circumpolar Soil Carbon Database, particularly as the data may include some near-surface biomass components because the distinction between soil organic matter and live plant material (e.g. fine roots) is methodologically challenging.

Post-thaw carbon vulnerability depends on organic matter sources and histories, redox conditions, moisture, and temperature controlling mineralization versus export. Soil order creates distinct vulnerabilities: Histels contain labile compounds under anoxic conditions, Turbels bury undecomposed material through cryoturbation, while Orthels contain more processed organic matter that underwent surface decomposition before freezing, potentially reducing immediate vulnerability but creating uncertainty about long-term stability [60]. Forest type and wetland-upland gradients further modulate decomposition rates and stabilization mechanisms.

Reducing projection uncertainties requires improved process understanding and model capabilities. Advances in representing vegetation-permafrost feedbacks require explicit treatment of canopy radiation partitioning, snow-vegetation insulation effects, and organic layer dynamics [61, 62]. Enhanced snow physics and soil thermal modules would improve ground thermal regime simulations [63–66]. Integrating these processes with vegetation dynamics and disturbance regimes is critical for capturing forest-permafrost interactions [4, 61].

Several limitations affect interpretation of these PFT-specific patterns. The canopy's insulating effect on ALT varied by PFT, with DBF showing the strongest reduction. ENF exhibited moderate effects, while DNF showed consistently weaker impacts across regions. However, (1) unequal sample sizes across PFT classes may affect representativeness, and (2) we did not account for spatial autocorrelation between nearby stands of the same PFT. These factors influence the apparent strength of PFT-specific effects and their regional patterns.

Our analysis stratifies results by current Köppen climate zones to isolate permafrost response while acknowledging that this approach does not fully capture interacting feedback mechanisms. This stratification introduces uncertainty because climate zones themselves are dynamic under projected warming. Arctic and subarctic regions are projected to experience strong warming that will move climate zones. Arctic tundra climates (ET) are expected to contract, replaced largely by subarctic boreal climates (Dfc). Under all medium to high emission scenarios, subarctic boreal zones (mostly Dfc) will shift toward warmer boreal and temperate wet climates (Dfb). [67]. Overall, the future climate distribution will be dominated mainly by Dfc, Dfb, and Dfa climate zones as Arctic amplification progresses. As climate zones migrate geographically, the vegetation-permafrost relationships we observe within current climate zones may not remain stable, and existing forests will experience novel climatic conditions that alter canopy-snow-permafrost interactions.

Reducing uncertainties requires: (1) standardized deep soil sampling beyond 1 m across soil orders and forest types; (2) integrated SOC age profiling with disturbance history and spatial mapping; (3) coordinated observations from underrepresented forested permafrost regions; and (4) coupled model development linking canopy-snow-permafrost processes with vegetation succession and disturbance dynamics [61]. By isolating permafrost as the response variable we do not capture all the different feedback mechanisms in play but gain process understanding with the aim to parameterize the biogeophysical impact of canopies on permafrost for implementation in land surface models.

S4.5 Forest management

Although forest diversification can buffer against climate uncertainty while enhancing structural and functional diversity [68], our findings suggest that management priorities should emphasize maintaining sparse canopy cover rather than optimizing canopy density, productivity, or specific PFT compositions. Even if shifts toward high-productivity deciduous broadleaf taxa does not enhance soil carbon storage capacity directly [48], the hydrothermal protection afforded by any continuous canopy structure remains valuable for limiting SOC mobilization. From a management perspective, maintaining sparse, low-density canopies may offer additional resilience benefits under projected climate scenarios, particularly regarding drought tolerance, while preserving the critical shading function that protects substantial permafrost carbon pools from thaw-induced mobilization. Lowering stand density through thinning has been demonstrated to increase drought resistance and resilience at both tree and stand levels [69], reducing fire-proneness, with thinned forests exhibiting reduced canopy water stress and lower temperature increases during drought events compared to unthinned stands [70]. Meta-analyses confirm that thinning enhances forest resilience and resistance to multiple stressors including drought, pests, and fire, with benefits operating through reduced competition for water and decreased stand-level transpiration [71, 72]. Recent evidence from managed boreal landscapes indicates that drought responses vary with stand structure, with composition and density playing critical roles in carbon sink stability [73]. This approach aligns with adaptive management frameworks that prioritize ecosystem function preservation over structural optimization under increasing disturbance pressures [68], accommodating the amplifying uncertainties of climate change on boreal forest systems. Strategies to preserve key ecosystem functions, such as the thermal canopy-buffering of permafrost, include partial cutting and continuous cover forestry, which maintain multi-aged, structurally diverse canopies, or natural disturbance-based management, mimicking natural mortality patterns [74, 75].

S5 Model setup

Table 4 Overview of model parameters and constants.

Parameter	Symbol	Value	Unit	Source
CryoGrid soil parameters				
Density falling snow	ρ_{snow}	300	kg m^{-3}	[76]
Albedo ground	α	0.3		[77]
Roughness length	z_0	0.001	m	[78]
Roughness length snow	$z_{0\text{snow}}$	0.0001	m	[79]
Geothermal heat flux	F_{lb}	0.05	W m^{-2}	[78]
Thermal conductivity, mineral	$k_{\min}$	3.0	$\text{W m}^{-1}\text{ K}^{-1}$	[78]
Emissivity	ϵ	0.99		[80]
Root depth	D_T	0.2	m	[77]
Evaporation depth	D_E	0.1	m	[81]
Hydraulic conductivity	K	1×10^{-5}	m s^{-1}	[79]
Physical constants				
von Krmn constant	κ	0.4		
Freezing point of water	T_0	273.15	K	
Latent heat of vaporization	L_v	2.501×10^6	J kg^{-1}	
Molecular mass of water	M_w	18.016×10^{-3}	kg mol^{-1}	
Molecular mass of dry air	M_d	28.966×10^{-3}	kg mol^{-1}	
Specific heat, dry air	c_p	1004.64	$\text{J kg}^{-1}\text{ K}^{-1}$	
Density of fresh water	ρ_w	1000	kg m^{-3}	
Latent heat of fusion	L_f	0.334×10^6	J kg^{-1}	
Thermal conductivity of water	k_w	0.57	$\text{W m}^{-1}\text{ K}^{-1}$	
Thermal conductivity of ice	k_i	2.2	$\text{W m}^{-1}\text{ K}^{-1}$	
Kinematic viscosity of air (0 °C, 1013.25 hPa)	ν	1.33×10^{-5}	$\text{m}^2\text{ s}^{-1}$	
Specific heat, water vapor	c_{pv}	1810	$\text{J kg}^{-1}\text{ K}^{-1}$	
Multilayer canopy parameters				
Leaf angle dep. from spherical		0.01		Table 3, [82]
Leaf reflectance (VIS/NIR)		0.07/0.35		Table 3, [82]
Stem reflectance (VIS/NIR)		0.16/0.39		Table 2.8, [83]
Leaf transmittance (VIS/NIR)		0.05/0.10		Table 3, [82]
Stem transmittance (VIS/NIR)		0.001/0.001		Table 2.8, [83]
Photosynthetic pathway		C3		Table 6, [84]
Leaf emissivity		0.98		Table 3, [82]
Quantum efficiency		0.06	$\mu\text{mol}_{\text{CO2}}/\mu\text{mol}_{\text{photon}}$	Table 6, [84]
Ball-Berry intercept (g0)		0.01	$\text{mol}_{\text{H2O}}/\text{m}^2/\text{s}$	
Leaf dimension		0.04	m	Table 5, [84]
Momentum roughness length ratio		0.055		Table 5, [84]
Displacement height ratio		0.67		Table 5, [84]
Root distribution (a/b)		7.0/2.0		Table 5, [84]
Min. vapor pressure deficit		100	Pa	[85]
Plant capacitance		2500	$\text{mmol}_{\text{H2O}}/\text{m}^2/\text{MPa}$	Table 3, [82]
Minimum leaf water potential		−2	MPa	Table 3, [82]
Stem hydraulic conductance		4	$\text{mmol}_{\text{H2O}}/\text{m}^2/\text{s}/\text{MPa}$	Table 3, [82]
Atmospheric CO_2		380	$\mu\text{mol mol}^{-1}$	
Atmospheric O_2		209	mmol mol^{-1}	
Soil evaporative resistance		3362	s m^{-1}	[76]
Specific heat, dry-wet soil		1396	$\text{J kg}^{-1}\text{ K}^{-1}$	Eq. 6.90, [86]
Specific heat capacity, H_2O		4188	$\text{J kg}^{-1}\text{ K}^{-1}$	Table 2.6, [86]
Fine root biomass		500	$\text{g}_{\text{bio}}/\text{m}^2$	Table 3, [76]
Leaf drag coefficient		0.25		Eq. 16.20, [85]
Foliage clumping index		0.7		Eq. 14.12, [85]

Table 5 PFT-specific parameters for deciduous needleleaf (DNF), evergreen needleleaf (ENF), and deciduous broadleaf (DBF) PFTs.

Parameter	**DNF**	**ENF**	**DBF**	**Unit**
Max. carboxylation rate at 25 °C	39.1	62.6	57.7	$\mu mol\, m^{-2}\, s^{-1}$
Specific leaf area (TOC)	0.024	0.008	0.030	m^2/g_C
Ball-Berry slope (g1)	6	6	9	

Table 6 Overview of the forested (top) and bare ground (bottom) setups.

Depth [m]	Mineral θ_m	Organic θ_o	Porosity/Water/Ice θ_w^0	Soil type	Comment
0–0.08	0	0.2	0.8	Peat	Litter layer
0.09–0.16	0.1	0.2	0.7	Clay	Organic layer
0.17–1.0	0.4	0	0.6	Clay	Mineral layer
1.1–10.0	0.4	0	0.6	Clay	Mineral layer
10.1–100	0.97	0	0.03	Sand	Mineral layer

Depth [m]	Mineral θ_m	Organic θ_o	Porosity/Water/Ice θ_w^0	Soil type	Comment
0–0.04	0.4	0.1	0.5	Peat	Organic layer
0.05–0.1	0.6	0	0.4	Clay	Mineral layer
0.11–1.0	0.6	0	0.4	Clay	Mineral layer
1.1–10.0	0.6	0	0.4	Clay	Mineral layer
10.1–100	0.97	0	0.03	Sand	Mineral layer

References

[1] Shiklomanov, N., Streletskiy, D., Nelson, F.: Northern hemisphere component of the global circumpolar active layer monitoring (calm) program. In: Proceedings of the 10th International Conference on Permafrost, pp. 377–382 (2012). https://www.researchgate.net/publication/269932332

[2] Westermann, S., Barboux, C., Bartsch, A., Delaloye, R., Grosse, G., Heim, B., Hugelius, G., Irrgang, A., Kb, A.M., Matthes, H., Nitze, I., Pellet, C., Seifert, F.M., Strozzi, T., Wegmller, U., Wieczorek, M., Wiesmann, A.: ESA Permafrost Climate Change Initiative (Permafrost cci): Permafrost active layer thickness for the Northern Hemisphere, v4.0. NERC EDS Centre for Environmental Data Analysis (2024). https://dx.doi.org/10.5285/d34330ce3f604e368c06d76de1987ce5

[3] Langer, M., Nitzbon, J., Groenke, B., Assmann, L.-M., Deimling, T.S., Stuenzi, S.M., Westermann, S.: The evolution of arctic permafrost over the last 3centuries from ensemble simulations with the cryogridlite permafrost model. The Cryosphere **18**, 363–385 (2024) https://doi.org/10.5194/tc-18-363-2024

[4] Obu, J., Westermann, S., Bartsch, A., Berdnikov, N., Christiansen, H.H., Dashtseren, A., Delaloye, R., Elberling, B., Etzelmller, B., Kholodov, A., Khomutov, A., Kb, A., Leibman, M.O., Lewkowicz, A.G., Panda, S.K., Romanovsky, V., Way, R.G., Westergaard-Nielsen, A., Wu, T., Yamkhin, J., Zou, D.: Northern Hemisphere permafrost map based on TTOP modelling for 20002016 at 1km2 scale. Elsevier B.V. (2019). https://doi.org/10.1016/j.earscirev.2019.04.023

[5] Talucci, A.C., Loranty, M.M., Holloway, J.E., Rogers, B.M., Alexander, H.D., Baillargeon, N., Baltzer, J.L., Berner, L.T., Breen, A., Brodt, L., Buma, B., Dean, J., Delcourt, C.J.F., Diaz, L.R., Dieleman, C.M., Douglas, T.A., Frost, G.V., Gaglioti, B.V., Hewitt, R.E., Hollingsworth, T., Jorgenson, M.T., Lara,

M.J., Loehman, R.A., Mack, M.C., Manies, K.L., Minions, C., Natali, S.M., O'Donnell, J.A., Olefeldt, D., Paulson, A.K., Rocha, A.V., Saperstein, L.B., Shestakova, T.A., Sistla, S., Sizov, O., Soromotin, A., Turetsky, M.R., Veraverbeke, S., Walvoord, M.A.: Permafrostwildfire interactions: active layer thickness estimates for paired burned and unburned sites in northern high latitudes. Earth System Science Data **17**, 2887–2909 (2025) https://doi.org/10.5194/essd-17-2887-2025

[6] Brown, J., Jr., O.J.F., Heginbottom, J.A., Melnikov, E.S.: Circum-arctic map of permafrost and ground-ice conditions, version 2. Technical report, National Snow and Ice Data Center/World Data Center for Glaciology (2002). https://doi.org/10.3133/cp45 . https://nsidc.org/data/ggd318

[7] Hugelius, G., Tarnocai, C., Broll, G., Canadell, J.G., Kuhry, P., Swanson, D.K.: The northern circumpolar soil carbon database: Spatially distributed datasets of soil coverage and soil carbon storage in the northern permafrost regions. Earth System Science Data **5**, 3–13 (2013) https://doi.org/10.5194/essd-5-3-2013

[8] Strauss, J., Laboor, S., Schirrmeister, L., Fedorov, A.N., Fortier, D., Froese, D., Fuchs, M., Gnther, F., Grigoriev, M., Harden, J., Hugelius, G., Jongejans, L.L., Kanevskiy, M., Kholodov, A., Kunitsky, V., Kraev, G., Lozhkin, A., Rivkina, E., Shur, Y., Siegert, C., Spektor, V., Streletskaya, I., Ulrich, M., Vartanyan, S., Veremeeva, A., Anthony, K.W., Wetterich, S., Zimov, N., Grosse, G.: Database of Ice-Rich Yedoma Permafrost Version 2 (IRYP v2) [dataset]. PANGAEA (2022). https://doi.org/10.1594/PANGAEA.940078

[9] Mark, F., Damien, S.-M.: Mcd12q1 modis/terra+aqua land cover type yearly l3 global 500m sin grid. nasa lp daac. (2015)

[10] Peplau, T., Schroeder, J., Gregorich, E., Poeplau, C.: Subarctic soil carbon losses after deforestation for agriculture depend on permafrost abundance. Global

Change Biology **28**, 5227–5242 (2022) https://doi.org/10.1111/GCB.16307

[11] Grnzweig, J.M., Valentine, D.W., Chapin, F.S.: Successional changes in carbon stocks after logging and deforestation for agriculture in interior alaska: Implications for boreal climate feedbacks. Ecosystems **18**, 132–145 (2015) https://doi.org/10.1007/s10021-014-9817-x

[12] Grnzweig, J.M., Sparrow, S.D., Yakir, D., Chapin, F.S.: Impact of agricultural landuse change on carbon storage in boreal alaska. Global Change Biology **10**, 452–472 (2004) https://doi.org/10.1111/j.1365-2486.2004.00738.x

[13] Unc, A., Altdorff, D., Abakumov, E., Adl, S., Baldursson, S., Bechtold, M., Cattani, D.J., Firbank, L.G., Grand, S., Gujnsdttir, M., Kallenbach, C., Kedir, A.J., Li, P., McKenzie, D.B., Misra, D., Nagano, H., Neher, D.A., Niemi, J., Oelbermann, M., Lehmann, J.O., Parsons, D., Quideau, S., Sharkhuu, A., Smreczak, B., Sorvali, J., Vallotton, J.D., Whalen, J.K., Young, E.H., Zhang, M., Borchard, N.: Expansion of agriculture in northern cold-climate regions: A cross-sectoral perspective on opportunities and challenges. Frontiers in Sustainable Food Systems **5** (2021) https://doi.org/10.3389/fsufs.2021.663448

[14] Izbicki, B., Walker, X.J., Alexander, H.D., Borth, E., Hewitt, R.E., Zimov, N., Mack, M.C.: Wildfire and permafrost thaw reduce c pools and diminish carbon sequestration potential in yedoma surface soils. Journal of Geophysical Research: Biogeosciences **130** (2025) https://doi.org/10.1029/2024JG008631

[15] Hensgens, G., Laudon, H., Johnson, M.S., Berggren, M.: The undetected loss of aged carbon from boreal mineral soils. Scientific Reports **11**, 1–10 (2021) https://doi.org/10.1038/S41598-021-85506-W;SUBJMETA

[16] Scholten, R.C., Veraverbeke, S., Chen, Y., Randerson, J.T.: Spatial variability in

arcticboreal fire regimes influenced by environmental and human factors. Nature Geoscience (2024) https://doi.org/10.1038/s41561-024-01505-2

[17] Li, X., Sun, L., Han, Y.: Effects of Wildfires on Soil Organic Carbon in Boreal Permafrost Regions: A Review. John Wiley and Sons Ltd (2024). https://doi.org/10.1002/ppp.2247

[18] Janssen, T.A.J., Veraverbeke, S.: What are the limits to the growth of boreal fires? Global Change Biology **31** (2025) https://doi.org/10.1111/gcb.70130

[19] Jain, P., Barber, Q.E., Taylor, S.W., Whitman, E., Acuna, D.C., Boulanger, Y., Chavards, R.D., Chen, J., Englefield, P., Flannigan, M., Girardin, M.P., Hanes, C.C., Little, J., Morrison, K., Skakun, R.S., Thompson, D.K., Wang, X., Parisien, M.-A.: Drivers and impacts of the record-breaking 2023 wildfire season in canada. Nature Communications **15**, 6764 (2024) https://doi.org/10.1038/s41467-024-51154-7

[20] Veraverbeke, S., Janssen, T.A.J., Brambleby, E., Jones, M., Zoletto, B., Sande, M.T.: Lightning impacts on global forest and carbon dynamics: Current understanding and knowledge gaps. Global Change Biology **31** (2025) https://doi.org/10.1111/gcb.70179

[21] Foster, A.C., Armstrong, A.H., Shuman, J.K., Shugart, H.H., Rogers, B.M., Mack, M.C., Goetz, S.J., Ranson, K.J.: Importance of tree- and species-level interactions with wildfire, climate, and soils in interior alaska: Implications for forest change under a warming climate. Ecological Modelling **409**, 108765 (2019) https://doi.org/10.1016/J.ECOLMODEL.2019.108765

[22] Dsouza, K.B., Ofosu, E., Salkeld, J., Boudreault, R., Moreno-Cruz, J., Leonenko, Y.: Assessing the climate benefits of afforestation in the canadian northern boreal

and southern arctic. Nature Communications 2025 16:1 **16**, 1–19 (2025) https://doi.org/10.1038/s41467-025-56699-9

[23] Besnard, S., Heinrich, V.H.A., Carvalhais, N., Ciais, P., Herold, M., Luijkx, I., Peters, W., Suarez, D.R., Santoro, M., Yang, H.: Global covariation of forest age transitions with the net carbon balance. Nature Ecology & Evolution (2025) https://doi.org/10.1038/s41559-025-02821-5

[24] Yi, S., Woo, M.-k., Arain, M.A.: Impacts of peat and vegetation on permafrost degradation under climate warming. Geophysical Research Letters **34** (2007) https://doi.org/10.1029/2007GL030550

[25] Fisher, J.P., Estop-Aragons, C., Thierry, A., Charman, D.J., Wolfe, S.A., Hartley, I.P., Murton, J.B., Williams, M., Phoenix, G.K.: The influence of vegetation and soil characteristics on active-layer thickness of permafrost soils in boreal forest. Global Change Biology **22**, 3127–3140 (2016) https://doi.org/10.1111/gcb.13248

[26] Stuenzi, S.M., Kruse, S., Boike, J., Herzschuh, U., Oehme, A., Pestryakova, L.A., Westermann, S., Langer, M.: Thermohydrological impact of forest disturbances on ecosystemprotected permafrost. Journal of Geophysical Research: Biogeosciences **127** (2022) https://doi.org/10.1029/2021JG006630

[27] Walker, X.J., Baltzer, J.L., Cumming, S.G., Day, N.J., Johnstone, J.F., Rogers, B.M., Solvik, K., Turetsky, M.R., Mack, M.C.: Soil organic layer combustion in boreal black spruce and jack pine stands of the northwest territories, canada. International Journal of Wildland Fire **27**, 125–134 (2018) https://doi.org/10.1071/WF17095

[28] Waldrop, M.P., McFarland, J.W., Manies, K.L., Leewis, M.C., Blazewicz, S.J., Jones, M.C., Neumann, R.B., Keller, J.K., Cohen, L., Euskirchen, E.S., Edgar,

C., Turetsky, M.R., Cable, W.L.: Carbon fluxes and microbial activities from boreal peatlands experiencing permafrost thaw. Journal of Geophysical Research: Biogeosciences **126**, 2020–005869 (2021) https://doi.org/10.1029/2020JG005869

[29] Webb, E.E., Alexander, H.D., Paulson, A.K., Loranty, M.M., DeMarco, J., Talucci, A.C., Spektor, V., Zimov, N., Lichstein, J.W.: Fire-induced carbon loss and tree mortality in siberian larch forests. Geophysical Research Letters **51**, 2023–105216 (2024) https://doi.org/10.1029/2023GL105216

[30] Anyomi, K.A., Mitchell, S.J., Ruel, J.C.: Windthrow modelling in old-growth and multi-layered boreal forests. Ecological Modelling **327**, 105–114 (2016) https://doi.org/10.1016/J.ECOLMODEL.2016.02.003

[31] Seidl, R., Thom, D., Kautz, M., Martin-Benito, D., Peltoniemi, M., Vacchiano, G., Wild, J., Ascoli, D., Petr, M., Honkaniemi, J., Lexer, M.J., Trotsiuk, V., Mairota, P., Svoboda, M., Fabrika, M., Nagel, T.A., Reyer, C.P.O.: Forest disturbances under climate change. Nature Climate Change **7**, 395–402 (2017) https://doi.org/10.1038/nclimate3303

[32] Kautz, M., Meddens, A.J.H., Hall, R.J., Arneth, A.: Biotic disturbances in northern hemisphere forests a synthesis of recent data, uncertainties and implications for forest monitoring and modelling. Global Ecology and Biogeography **26**, 533–552 (2017) https://doi.org/10.1111/GEB.12558

[33] Mekonnen, Z.A., Riley, W.J., Randerson, J.T., Grant, R.F., Rogers, B.M.: Expansion of high-latitude deciduous forests driven by interactions between climate warming and fire. Nature Plants **5**, 952–958 (2019) https://doi.org/10.1038/s41477-019-0495-8

[34] Loranty, M.M., Lieberman-Cribbin, W., Berner, L.T., Natali, S.M., Goetz, S.J.,

Alexander, H.D., Kholodov, A.L.: Spatial variation in vegetation productivity trends, fire disturbance, and soil carbon across arctic-boreal permafrost ecosystems. Environmental Research Letters **11**, 095008 (2016) https://doi.org/10.1088/1748-9326/11/9/095008

[35] Gibson, C.M., Chasmer, L.E., Thompson, D.K., Quinton, W.L., Flannigan, M.D., Olefeldt, D.: Wildfire as a major driver of recent permafrost thaw in boreal peatlands. Nature Communications **9** (2018) https://doi.org/10.1038/s41467-018-05457-1

[36] Schuur, E.A.G., Vogel, J.G., Crummer, K.G., Lee, H., Sickman, J.O., Osterkamp, T.E.: The effect of permafrost thaw on old carbon release and net carbon exchange from tundra. Nature **459**, 556–559 (2009) https://doi.org/10.1038/nature08031

[37] Schuur, E.A.G., Abbott, B.W., Commane, R., Ernakovich, J., Euskirchen, E., Hugelius, G., Grosse, G., Jones, M., Koven, C., Leshyk, V., Lawrence, D., Loranty, M.M., Mauritz, M., Olefeldt, D., Natali, S., Rodenhizer, H., Salmon, V., Schdel, C., Strauss, J., Treat, C., Turetsky, M.: Permafrost and climate change: Carbon cycle feedbacks from the warming arctic. Annual Review of Environment and Resources **47**, 343–371 (2022) https://doi.org/10.1146/annurev-environ-012220-011847

[38] McGuire, A.D., Lawrence, D.M., Koven, C., Clein, J.S., Burke, E., Chen, G., Jafarov, E., MacDougall, A.H., Marchenko, S., Nicolsky, D., Peng, S., Rinke, A., Ciais, P., Gouttevin, I., Hayes, D.J., Ji, D., Krinner, G., Moore, J.C., Romanovsky, V., Schdel, C., Schaefer, K., Schuur, E.A.G., Zhuang, Q.: Dependence of the evolution of carbon dynamics in the northern permafrost region on the trajectory of climate change. Proceedings of the National Academy of Sciences **115**, 3882–3887 (2018) https://doi.org/10.1073/pnas.1719903115

[39] Finger, R.A., Turetsky, M.R., Kielland, K., Ruess, R.W., Mack, M.C., Euskirchen, E.S.: Effects of permafrost thaw on nitrogen availability and plantsoil interactions in a boreal alaskan lowland. Journal of Ecology **104**, 1542–1554 (2016) https://doi.org/10.1111/1365-2745.12639

[40] Ramm, E., Liu, C., Ambus, P., Butterbach-Bahl, K., Hu, B., Martikainen, P.J., Marushchak, M.E., Mueller, C.W., Rennenberg, H., Schloter, M., Siljanen, H.M.P., Voigt, C., Werner, C., Biasi, C., Dannenmann, M.: A review of the importance of mineral nitrogen cycling in the plant-soil-microbe system of permafrost-affected soilschanging the paradigm. Environmental Research Letters **17**, 013004 (2022) https://doi.org/10.1088/1748-9326/AC417E

[41] Pearson, R.G., Phillips, S.J., Loranty, M.M., Beck, P.S.A., Damoulas, T., Knight, S.J., Goetz, S.J.: Shifts in arctic vegetation and associated feedbacks under climate change. Nature Climate Change **3**, 673–677 (2013) https://doi.org/10.1038/nclimate1858

[42] Myers-Smith, I.H., Kerby, J.T., Phoenix, G.K., Bjerke, J.W., Epstein, H.E., Assmann, J.J., John, C., Andreu-Hayles, L., Angers-Blondin, S., Beck, P.S.A., Berner, L.T., Bhatt, U.S., Bjorkman, A.D., Blok, D., Bryn, A., Christiansen, C.T., Cornelissen, J.H.C., Cunliffe, A.M., Elmendorf, S.C., Forbes, B.C., Goetz, S.J., Hollister, R.D., Jong, R., Loranty, M.M., Macias-Fauria, M., Maseyk, K., Normand, S., Olofsson, J., Parker, T.C., Parmentier, F.-J.W., Post, E., Schaepman-Strub, G., Stordal, F., Sullivan, P.F., Thomas, H.J.D., Tmmervik, H., Treharne, R., Tweedie, C.E., Walker, D.A., Wilmking, M., Wipf, S.: Complexity revealed in the greening of the arctic. Nature Climate Change **10**, 106–117 (2020) https://doi.org/10.1038/s41558-019-0688-1

[43] Mack, M.C., Walker, X.J., Johnstone, J.F., Alexander, H.D., Melvin, A.M., Jean,

M., Miller, S.N.: Carbon loss from boreal forest wildfires offset by increased dominance of deciduous trees. Science **372**, 280–283 (2021) https://doi.org/10.1126/science.abf3903

[44] Keuper, F., Wild, B., Kummu, M., Beer, C., Blume-Werry, G., Fontaine, S., Gavazov, K., Gentsch, N., Guggenberger, G., Hugelius, G., Jalava, M., Koven, C., Krab, E.J., Kuhry, P., Monteux, S., Richter, A., Shahzad, T., Weedon, J.T., Dorrepaal, E.: Carbon loss from northern circumpolar permafrost soils amplified by rhizosphere priming. Nature Geoscience **13**, 560–565 (2020) https://doi.org/10.1038/S41561-020-0607-0;TECHMETA

[45] Kropp, H., Loranty, M.M., Natali, S.M., Kholodov, A.L., Rocha, A.V., Myers-Smith, I.H., Abbott, B.W., Abermann, J., Blanc-Betes, E., Blok, D., Blume-Werry, G., Boike, J., Breen, A.L., Cahoon, S.M.P., Christiansen, C.T., Douglas, T.A., Epstein, H.E., Frost, G.V., Goeckede, M., Hye, T.T., Mamet, S.D., O'Donnell, J.A., Olefeldt, D., Phoenix, G.K., Salmon, V.G., Sannel, A.B.K., Smith, S.L., Sonnentag, O., Vaughn, L., Williams, M., Elberling, B., Gough, L., Hjort, J., Lafleur, P.M., Euskirchen, E.S., Heijmans, M., Humphreys, E.R., Iwata, H., Jones, B.M., Jorgenson, T., Grnberg, I., Kim, Y., Laundre, J., Mauritz, M., Michelsen, A., Schaepman-Strub, G., Tape, K.D., Ueyama, M., Lee, B.-Y., Langley, K., Lund, M.: Shallow soils are warmer under trees and tall shrubs across arctic and boreal ecosystems. Environmental Research Letters **16** (2021) https://doi.org/10.1088/1748-9326/abc994

[46] Mekonnen, Z.A., Riley, W.J., Berner, L.T., Bouskill, N.J., Torn, M.S., Iwahana, G., Breen, A.L., Myers-Smith, I.H., Criado, M.G., Liu, Y., Euskirchen, E.S., Goetz, S.J., Mack, M.C., Grant, R.F.: Arctic tundra shrubification: a review of mechanisms and impacts on ecosystem carbon balance. Environmental Research Letters **16**, 053001 (2021) https://doi.org/10.1088/1748-9326/ABF28B

[47] Heijmans, M.M.P.D., Magnsson, R., Lara, M.J., Frost, G.V., Myers-Smith, I.H., Huissteden, J., Jorgenson, M.T., Fedorov, A.N., Epstein, H.E., Lawrence, D.M., Limpens, J.: Tundra vegetation change and impacts on permafrost. Nature Reviews Earth & Environment 2022 3:1 **3**, 68–84 (2022) https://doi.org/10.1038/s43017-021-00233-0

[48] Hartley, I.P., Garnett, M.H., Sommerkorn, M., Hopkins, D.W., Fletcher, B.J., Sloan, V.L., Phoenix, G.K., Wookey, P.A.: A potential loss of carbon associated with greater plant growth in the european arctic. Nature Climate Change **2**, 875–879 (2012) https://doi.org/10.1038/NCLIMATE1575;SUBJMETA

[49] Burke, K.D., Williams, J.W., Chandler, M.A., Haywood, A.M., Lunt, D.J., Otto-Bliesner, B.L.: Pliocene and eocene provide best analogs for near-future climates. Proceedings of the National Academy of Sciences **115**, 13288–13293 (2018) https://doi.org/10.1073/pnas.1809600115

[50] Wulder, M.A., Hermosilla, T., White, J.C., Coops, N.C.: Biomass status and dynamics over canadas forests: Disentangling disturbed area from associated aboveground biomass consequences. Environmental Research Letters **15**, 094093 (2020) https://doi.org/10.1088/1748-9326/ab8b11

[51] Rotbarth, R., Nes, E.H., Scheffer, M., Holmgren, M.: Boreal forests are heading for an open state. Proceedings of the National Academy of Sciences of the United States of America **122**, 2404391121 (2025) https://doi.org/10.1073/pnas.2404391121

[52] Park, S.-W., Mun, J.-H., Lee, H., Steinert, N.J., An, S.-I., Shin, J., Kug, J.-S.: Continued permafrost ecosystem carbon loss under net-zero and negative emissions. Science Advances **11** (2025) https://doi.org/10.1126/sciadv.adn8819

[53] Jobbgy, E.G., Jackson, R.B.: The vertical distribution of soil organic carbon and its relation to climate and vegetation. Ecological Applications **10**, 423–436 (2000) https://doi.org/10.1890/1051-0761(2000)010

[54] Tamocai, C., Canadell, J.G., Schuur, E.A.G., Kuhry, P., Mazhitova, G., Zimov, S.: Soil organic carbon pools in the northern circumpolar permafrost region. Global Biogeochemical Cycles **23** (2009) https://doi.org/10.1029/2008GB003327

[55] Jorgenson, M.T., Harden, J., Kanevskiy, M., O'Donnell, J., Wickland, K., Ewing, S., Manies, K., Zhuang, Q., Shur, Y., Striegl, R., Koch, J.: Reorganization of vegetation, hydrology and soil carbon after permafrost degradation across heterogeneous boreal landscapes. Environmental Research Letters **8**, 035017 (2013) https://doi.org/10.1088/1748-9326/8/3/035017

[56] Hugelius, G., Strauss, J., Zubrzycki, S., Harden, J.W., Schuur, E.A.G., Ping, C.L., Schirrmeister, L., Grosse, G., Michaelson, G.J., Koven, C.D., O'Donnell, J.A., Elberling, B., Mishra, U., Camill, P., Yu, Z., Palmtag, J., Kuhry, P.: Estimated stocks of circumpolar permafrost carbon with quantified uncertainty ranges and identified data gaps. Biogeosciences **11**, 6573–6593 (2014) https://doi.org/10.5194/bg-11-6573-2014

[57] Pan, Y., Birdsey, R.A., Fang, J., Houghton, R., Kauppi, P.E., Kurz, W.A., Phillips, O.L., Shvidenko, A., Lewis, S.L., Canadell, J.G., Ciais, P., Jackson, R.B., Pacala, S.W., McGuire, A.D., Piao, S., Rautiainen, A., Sitch, S., Hayes, D.: A large and persistent carbon sink in the world's forests. Science **333**, 988–993 (2011) https://doi.org/10.1126/SCIENCE.1201609/ASSET/3636D6B8-BA93-4053-8457-4971C2A7EDC2/ASSETS/GRAPHIC/333_988_F1.JPEG

[58] Bradshaw, C.J., Warkentin, I.G.: Global estimates of boreal forest carbon stocks

and flux. Global and Planetary Change **128**, 24–30 (2015) https://doi.org/10.1016/j.gloplacha.2015.02.004

[59] Shorohova, E., Kapitsa, E., Ruokolainen, A., Romashkin, I., Kazartsev, I.: Types and rates of decomposition of larix sibirica trees and logs in a mixed european boreal old-growth forest. Forest Ecology and Management **439**, 173–180 (2019) https://doi.org/10.1016/j.foreco.2019.03.007

[60] Harden, J.W., Koven, C.D., Ping, C.L., Hugelius, G., McGuire, A.D., Camill, P., Jorgenson, T., Kuhry, P., Michaelson, G.J., O'Donnell, J.A., Schuur, E.A.G., Tarnocai, C., Johnson, K., Grosse, G.: Field information links permafrost carbon to physical vulnerabilities of thawing. Geophysical Research Letters **39**, 15704 (2012) https://doi.org/10.1029/2012GL051958

[61] Steinert, N.J., Debolskiy, M.V., Burke, E.J., Garca-Pereira, F., Lee, H.: Evaluating permafrost definitions for global permafrost area estimates in cmip6 climate models. Environmental Research Letters **19**, 014033 (2023) https://doi.org/10.1088/1748-9326/AD10D7

[62] Luo, Z., Ji, D., Ahrens, B.: Assessing climate modeling uncertainties in the siberian frozen soil regions by contrasting cmip6 and ls3mip (2025) https://doi.org/10.5194/EGUSPHERE-2025-389

[63] Dankers, R., Burke, E.J., Price, J.: Simulation of permafrost and seasonal thaw depth in the jules land surface scheme. Cryosphere **5**, 773–790 (2011) https://doi.org/10.5194/TC-5-773-2011

[64] Ekici, A., Chadburn, S., Chaudhary, N., Hajdu, L.H., Marmy, A., Peng, S., Boike, J., Burke, E., Friend, A.D., Hauck, C., Krinner, G., Langer, M., Miller, P.A., Beer, C.: Site-level model intercomparison of high latitude and high altitude soil

thermal dynamics in tundra and barren landscapes. Cryosphere **9**, 1343–1361 (2015) https://doi.org/10.5194/tc-9-1343-2015

[65] Aalto, J., Karjalainen, O., Hjort, J., Luoto, M.: Statistical forecasting of current and future circum-arctic ground temperatures and active layer thickness. Geophysical Research Letters **45**, 4889–4898 (2018) https://doi.org/10.1029/2018GL078007

[66] Burke, E.J., Zhang, Y., Krinner, G.: Evaluating permafrost physics in the coupled model intercomparison project 6 (cmip6) models and their sensitivity to climate change. Cryosphere **14**, 3155–3174 (2020) https://doi.org/10.5194/TC-14-3155-2020,

[67] Beck, H.E., McVicar, T.R., Vergopolan, N., Berg, A., Lutsko, N.J., Dufour, A., Zeng, Z., Jiang, X., Dijk, A.I.J.M., Miralles, D.G.: High-resolution (1 km) kppen-geiger maps for 19012099 based on constrained cmip6 projections. Scientific Data **10**, 1–16 (2023) https://doi.org/10.1038/S41597-023-02549-6;SUBJMETA=106,2739,2786,2807,694,704;KWRD=ENVIRONMENTAL+HEALTH,PROJECTION+AND+PREDICTION

[68] Trivio, M., Potterf, M., Tijern, J., Ruiz-Benito, P., Burgas, D., Eyvindson, K., Blattert, C., Mnkknen, M., Duflot, R.: Enhancing resilience of boreal forests through management under global change: a review. Current Landscape Ecology Reports **8**, 103–118 (2023) https://doi.org/10.1007/s40823-023-00088-9

[69] Wotherspoon, A.R., Duchesne, L., Barrette, M., Houle, D.: Pre-commercial thinning could mitigate drought stress of black spruce stands. Forest Ecology and Management **517**, 120278 (2022) https://doi.org/10.1016/j.foreco.2022.120278

[70] Sankey, T., Tatum, J.: Thinning increases forest resiliency during unprecedented drought. Scientific Reports **12**, 9041 (2022) https://doi.org/10.1038/s41598-022-12982-z

[71] Willig, J., Schwarz, J., Comeau, P., Hartmann, H., Kohnle, U., Espelta, J.M., Mkinen, H., Ogaya, R., Peltoniemi, M., Penuelas, J., Roth, B., Ruiz-Peinado, R., Ruge, F., Bauhus, J.: No increased drought-related mortality after thinning: a meta-analysis. Annals of Forest Science **82**, 6 (2025) https://doi.org/10.1186/s13595-025-01278-7

[72] Chagnon, C., Dumont, S., Morin-Bernard, A., Jactel, H., Achim, A., Moreau, G.: Potential of thinning to increase forest resilience and resistance to drought, pest, windstorm and fire: A meta-analysis. Forest Ecology and Management **590**, 122788 (2025) https://doi.org/10.1016/j.foreco.2025.122788

[73] Martnez-Garca, E., Nilsson, M.B., Laudon, H., Lundmark, T., Fransson, J.E.S., Wallerman, J., Peichl, M.: Drought response of the boreal forest carbon sink is driven by understoreytree composition. Nature Geoscience **17**, 197–204 (2024) https://doi.org/10.1038/s41561-024-01374-9

[74] Girona, M.M.: Boreal Forests in the Face of Climate Change vol. 74. Springer, ??? (2023). https://doi.org/10.1007/978-3-031-15988-6

[75] Kuuluvainen, T., Angelstam, P., Frelich, L., Jgiste, K., Koivula, M., Kubota, Y., Lafleur, B., Macdonald, E.: Natural disturbance-based forest management: Moving beyond retention and continuous-cover forestry. Frontiers in Forests and Global Change **4** (2021) https://doi.org/10.3389/ffgc.2021.629020

[76] Stuenzi, S.M., Boike, J., Cable, W., Herzschuh, U., Kruse, S., Pestryakova, L.A., Deimling, T.S.V., Westermann, S., Zakharov, E.S., Langer, M.: Variability of the

surface energy balance in permafrost-underlain boreal forest. Biogeosciences **18**, 343–365 (2021) https://doi.org/10.5194/bg-18-343-2021

[77] Stuenzi, S.M., Boike, J., Westermann, S., Langer, M.: Boreal forest cover delays thermokarst onset in central siberia's yedoma deposits. Journal of Geophysical Research: Earth Surface **130**, 2024–007873 (2025) https://doi.org/10.1029/2024JF007873

[78] Westermann, S., Langer, M., Boike, J., Heikenfeld, M., Peter, M., Etzelmller, B., Krinner, G.: Simulating the thermal regime and thaw processes of ice-rich permafrost ground with the land-surface model cryogrid 3. Geoscientific Model Development **9**, 523–546 (2016) https://doi.org/10.5194/gmd-9-523-2016

[79] Boike, J., Nitzbon, J., Anders, K., Grigoriev, M., Bolshiyanov, D., Langer, M., Lange, S., Bornemann, N., Morgenstern, A., Schreiber, P., Wille, C., Chadburn, S., Gouttevin, I., Burke, E., Kutzbach, L.: A 16-year record (2002-2017) of permafrost, active-layer, and meteorological conditions at the samoylov island arctic permafrost research site, lena river delta, northern siberia: an opportunity to validate remote-sensing data and land surface, snow, and. Earth Syst. Sci. Data **11**, 261–299 (2019) https://doi.org/10.5194/essd-11-261-2019

[80] Langer, M., Westermann, S., Muster, S., Piel, K., Boike, J.: The surface energy balance of a polygonal tundra site in northern siberia - part 1: Spring to fall. Cryosphere **5**, 509–524 (2011) https://doi.org/10.5194/tc-5-509-2011

[81] Nitzbon, J., Langer, M., Westermann, S., Martin, L., Aas, K.S., Boike, J.: Pathways of ice-wedge degradation in polygonal tundra under different hydrological conditions. Cryosphere **13**, 1089–1123 (2019) https://doi.org/10.5194/tc-13-1089-2019

[82] Bonan, G.B., Williams, M., Fisher, R.A., Oleson, K.W.: Modeling stomatal conductance in the earth system: Linking leaf water-use efficiency and water transport along the soil-plant-atmosphere continuum. Geoscientific Model Development **7**, 2193–2222 (2014) https://doi.org/10.5194/gmd-7-2193-2014

[83] CLM: Community land model 5 (CLM5) manual [Computer software manual] (2018). https://escomp.github.io/ctsm-docs/versions/release-clm5.0/html/users_guide/index.html

[84] Bonan, G.B.: Ecological Climatology: Concepts and Applications, p. 678. Cambridge University Press, ??? (2002)

[85] Bonan, G.B.: Climate Change and Terrestrial Ecosystem Modeling. Cambridge University Press, ??? (2019). https://doi.org/10.1017/9781107339217

[86] Oleson, K.W., Lead, D.M.L., Bonan, G.B., Drewniak, B., Huang, M., Koven, C.D., Levis, S., Li, F., Riley, W.J., Subin, Z.M., Swenson, S.C., Thornton, P.E., Bozbiyik, A., Fisher, R., Heald, C.L., Kluzek, E., Lamarque, J.-F., Lawrence, P.J., Leung, L.R., Lipscomb, W., Muszala, S., Ricciuto, D.M., Sacks, W., Sun, Y., Tang, J., Yang, Z.-L.: Technical description of version 4.5 of the community land model (clm). In: Environmental Science, Engineering, Geography (2013). https://doi.org/10.5065/D6RR1W7M